MICROWAVE AND OPTICAL TECHNOLOGY LETTERS

EDITOR
Wenquan Che

South China University of Technology
School of Electronic and
Information Engineering

VOLUME 62 / NUMBER 2 FEBRUARY 2020

MICROWAVE AND OPTICAL TECHNOLOGY LETTERS ISSN: 0895-2477 (Print); ISSN 1098-2760 (Online) is published monthly by Wiley Subscription Services Inc., a Wiley Company, 111 River Street, Hoboken, NJ 07030-5774. Periodical Postage Paid at Hoboken, NJ and additional offices.

Postmaster: Send all address changes to MICROWAVE AND OPTICAL TECHNOLOGY LETTERS, John Wiley & Sons Inc., C/O The Sheridan Press, PO Box 465, Hanover, PA 17331 USA.

Aims and Scope

MICROWAVE AND OPTICAL TECHNOLOGY LETTERS provides quick publication (three- to six-month turnaround) of the most recent findings and achievements in high frequency technology, from RF to optical spectrum. The journal publishes original short papers and letters on theoretical, applied, and system results in the following areas:

RF, Microwave, and Millimeter Waves
Antennas and Propagation
Submillimeter-Wave and Infrared Technology
Optical Engineering

All papers are subject to peer review before publication.

Information for subscribers: MICROWAVE AND OPTICAL TECHNOLOGY LETTERS is published in 12 issues per year. Institutional subscription prices for 2020 are: Print & Online US$7110 (US), US$7527 (Rest ofWorld), €4859 (Europe), £3845 (UK). Prices are exclusive of tax. Asia-Pacific GST, Canadian GST/HST and European VAT will be applied at the appropriate rates. For more information on current tax rates, please go to www.wileyonlinelibrary.com/tax-vat. The price includes online access to the current and all online back files to January 1st 2014, where available. For other pricing options, including access information and terms and conditions, please visit www.wileyonlinelibrary.com/access.

Delivery Terms and Legal Title: Where the subscription price includes print issues and delivery is to the recipient's address, delivery terms are Delivered at Place (DAP); the recipient is responsible for paying any import duty or taxes. Title to all issues transfers FOB our shipping point, freight prepaid. We will endeavour to fulfill claims for missing or damaged copies within six months of publication, within our reasonable discretion and subject to availability.

Journal Customer Services: For ordering information, claims and any enquiry concerning your journal subscription please go to www.wileycustomerhelp.com/ask or contact your nearest office.

Americas: Email: cs-journals@wiley.com; Tel: +1 781 388 8598 or +1 800 835 6770 (Toll free in the USA & Canada).

Europe, Middle East and Africa: Email: cs-journals@wiley.com; Tel: +44 (0) 1865 778315.

Asia Pacific: Email: cs-journals@wiley.com; Tel: +65 6511 8000.

Japan: For Japanese speaking support, Email: cs-japan@wiley.com.

Visit our Online Customer Help available in 7 languages at www.wileycustomerhelp.com/ask

Back issues: Single issues from current and recent volumes are available at the current single issue price from cs-journals@wiley.com. Earlier issues may be obtained from Periodicals Service Company, 351 Fairview Avenue - Ste 300, Hudson, NY 12534, USA. Tel: +1 518 822-9300, Fax: +1 518 822-9305, Email: psc@periodicals.com

Author Reprints (50–500 copies): Order online: http://www.sheridanreprints.com/order-form.html; Email: Chris.Jones@sheridan.com

Manuscripts should be submitted online at: https://mc.manuscriptcentral.com/mop

Wiley's Corporate Citizenship initiative seeks to address the environmental, social, economic, and ethical challenges faced in our business and which are important to our diverse stakeholder groups. Since launching the initiative, we have focused on sharing our content with those in need, enchancing community philanthropy, reducing our carbon impact, creating global guidelines and best practices for paper use, establishing a vendor code of ethics, and engaging our colleagues and other stakeholders in our efforts.

Other correspondence should be addressed to: MICROWAVE AND OPTICAL TECHNOLOGY LETTERS, Publisher, c/o John Wiley & Sons, Inc., 111 River Street, Hoboken, NJ 07030. For submission instructions, subscription, and all other information visit: wileyonlinelibrary.com/journal/mop

View this journal online at wileyonlinelibrary.com/journal/mop
Printed in the USA by The Sheridan Group.
Production Editor: Erin Hernandez (email: jrnlprod_MOP@wiley.com).

This paper meets the requirements of ANSI/NISO Z39, 48-1992 (Permancence of Paper). ♾

MICROWAVE AND OPTICAL TECHNOLOGY LETTERS

VOLUME 62 / NUMBER 2 FEBRUARY 2020

Received: 14 May 2019
DOI: 10.1002/mop.32127

WILEY

RESEARCH ARTICLE

Palm tree coplanar Vivaldi antenna for near field radar application

N. Nurhayati[1] | **Alexandre M. De Oliveira**[2] | **João F. Justo**[3] | **Eko Setijadi**[4] | **Bagus E. Sukoco**[5] | **E. Endryansyah**[1]

[1]Department of Electrical Engineering, Universitas Negeri Surabaya, Surabaya, Indonesia

[2]Maxwell Laboratory of Microwave and Applied Electromag, Federal Institute of São Paulo, Cubatãoo, Brazil

[3]Department of Electronic Systems Engineering, Polytechnic School of the University of São Paulo, Brazil

[4]Department of Electrical Engineering, Institut Teknologi Sepuluh Nopember, Surabaya, Indonesia

[5]Pusat Penelitian Elektronika dan Telekomunikasi (PPET), Lembaga Ilmu Pengetahuan Indonesia (LIPI), Bandung, Indonesia

Correspondence
N. Nurhayati, Department of Electrical Engineering, Universitas Negeri Surabaya, Surabaya, Indonesia.
Email: nurhayati@unesa.ac.id

Abstract

The Vivaldi antenna is an ultra-wideband device that has high gain and directional radiation pattern. This paper performs a comparison of conventional, regular and exponential edges of a Palm Tree Vivaldi antenna that could operate in L and S band frequencies. The conventional coplanar Vivaldi antenna (C-CVA), regular coplanar Vivaldi antenna (R-CVA), exponential slot edge coplanar Vivaldi antenna (ESE-CVA), regular antipodal Vivaldi antenna (R-AVA) and exponential slot edge antipodal Vivaldi antenna (ESE-AVA), all with the same dimensions, are compared in terms of reflection coefficient and radiation pattern performance. Gain improvement is achieved as 6.22, 7.64, 7.90, 7.92, and 10.74 dB at 3 GHz respectively for R-AVA, ESE-AVA, Convetional - Coplanar Vivaldi Antenna, R-CVA, and ESE-CVA. The number, height, and opening rate of slot edges predispose current distribution and radiation pattern of CVA. Our results show that the exponential slot edge coplanar Vivaldi antenna provides the best gain and derives the best side lobe level, which confirmed the possibility of applying the Palm Tree technique to coplanar Vivaldi antennas, in addition to the antipodal ones, as originally proposed.

KEYWORDS

antipodal, coplanar, exponential slot, radiation pattern, Vivaldi

1 | INTRODUCTION

Vivaldi antenna is a simple and robust planar device, which has been the focus of recent intensive research, mostly due to its superior unique properties, it is compact, easy to manufacture, with small dimensions and high gain, and could be integrated directly in a circuit board.[1] As a result, it is suitable for many ultra-wideband (UWB) microwave applications. There are many applications for L and S bands, such as cell phone and wireless communication,[2] ground penetrating radar,[3] software defined and cognitive radios,[4] medical imaging and on-body telemetry,[5,6] astronomy,[7] satellite communication, surveillance and amateur radio. All such application needs reliable system mainly for antenna optimization as front end of telecommunication device.

Despite such features, the Vivaldi antenna still carries many shortcomings. The original antenna design has limitations, particularly on directivity and gain, such that a design optimization procedure is generally required for a specific application. Over the last few years, many strategies have been developed to improve those properties, for example by adding trapezoid lens,[8] using double antipodal structures,[9] and metamaterials.[10] However, all those solutions compromise the main constructive advantage, by increasing the final antenna dimensions and making the design more complex. Therefore, it is important to search for new design strategies, in order to overcome those limitations, but not compromising the original design simplicity. Recently, several investigations have explored the design of the slot edges on antipodal Vivaldi antennas (AVA),[11-16] using rectangular, straight slot and comb structure.

It has been shown that the exponential slot edge for AVA (ESE-AVA),[17] labeled as the Palm Tree antenna, has superior radiation patterns when compared to antennas with other slot edge designs.[18,19] This antenna simultaneously increases the gain, boosts the main lobe, and reduces the side lobe level (SLL), all without making the design more complex or increasing its volume. While investigations have so far explored the

design of the slot edge in antipodal configuration, a recent investigation has indicated that CVA could also benefit[20] from slot edge optimization,[21] in order to increase gain and enhance the main lobe of radiation patterns.

This investigation explores the design of slot edges on both AVA and CVA, and the resulting radiation properties for applications in L and S bands. We compare the reflection coefficient and radiation performance of Conventional Coplanar Vivaldi Antenna (C-CVA), Regular Coplanar Vivaldi Antenna (R-CVA), Exponential Slot Edge Coplanar Vivaldi Antenna (ESE-CVA), Regular Antipodal Vivaldi Antenna (R-AVA), and Exponential Slot Edge Antipodal Vivaldi Antenna (ESE-AVA), by keeping the geometry with the same dimensions. We also compare the effect of the number, height, and opening rate of slot edges to the radiation pattern and current distribution. From simulations and measurements, we find that CVA has better overall radiation pattern performance than AVA in L and S band frequency. Particularly, among all tested designs, the ESE-CVA provides the best gain at 10.74 dB and −7.14 of SLL. We also compare some near field measurement for CVA and AVA in different object. This manuscript is presented as follows: Section 2 presents the design procedure of the AVA and CVA, Section 3 presents results on the antenna performance, Section 4 presents experimental results specifically for the ESE-CVA, and finally Section 5 presents some concluding remarks.

2 | VIVALDI ANTENNA

We consider five types of Vivaldi antennas with the same dimensions as 1.25 λ and 1.25 λ at canter frequency, as shown in Figure 1 and with dimensions given in Table 1. Vivaldi antennas are simulated in L and S band frequency from 1-4 GHz with 2.5 GHz as center frequency to get reflection coefficient and radiation pattern performance.

The antennas are designed considering a FR4 substrate with permittivity of 4.6, and 1.6 mm of thickness and 0.035 mm of patch thickness. Although the antipodal and coplanar Vivaldi antennas have different feeding shapes, they have the same width of transmission line. All the parameters of exponential slot edge for both antennas have the same dimensions except for the transmission line and the part in the circle dash. The exponential tapered slot and exponential slot edge are designed by[15]:

$$y = C_1 e^{\mathrm{Rnx}} + C_2 \tag{1}$$

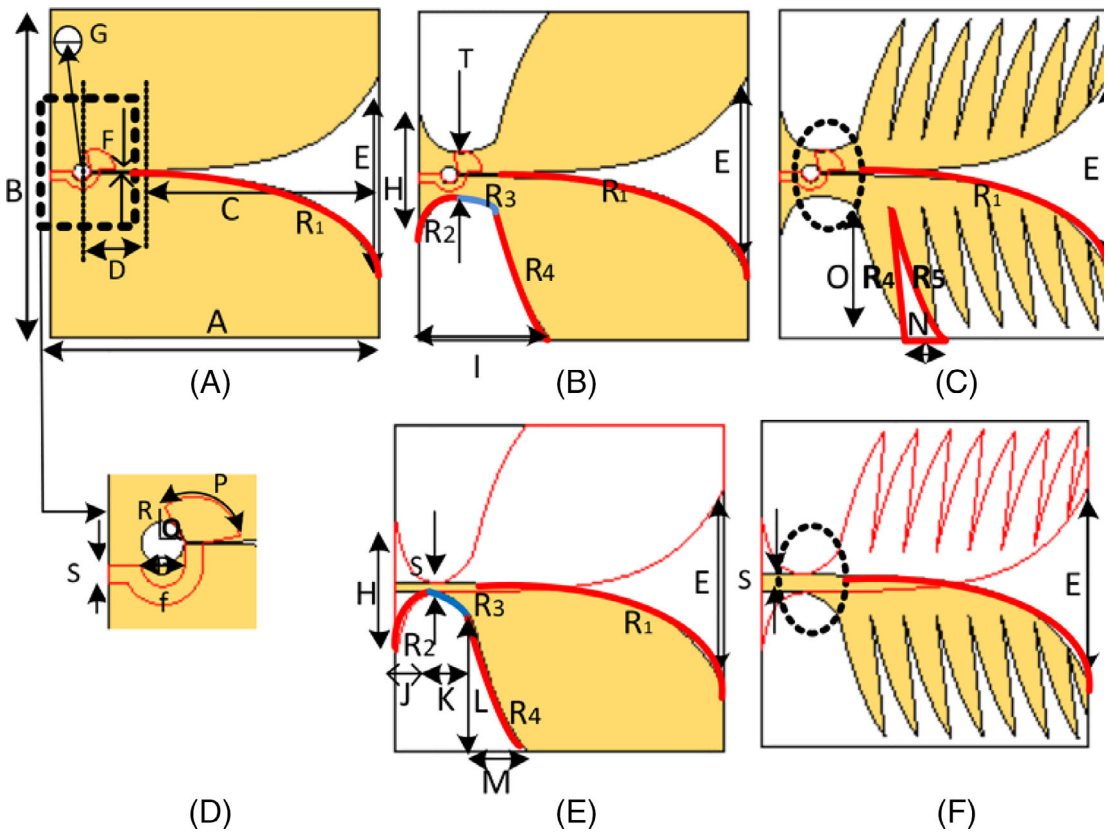

FIGURE 1 Antenna dimensions of A, C-CVA; B, R-CVA; C, ESE-CVA; D, feeding shape of CVA and *xyz* indicator, (E) R-AVA, and (F) ESE-AVA. C-CVA, conventional coplanar Vivaldi antenna; CVA, coplanar Vivaldi antenna; ESE-AVA, exponential slot edge antipodal Vivaldi antenna; ESE-CVA, exponential slot edge coplanar Vivaldi antenna; R-AVA, regular antipodal Vivaldi antenna; R-CVA, regular coplanar Vivaldi antenna [Color figure can be viewed at wileyonlinelibrary.com]

TABLE 1 Antenna parameters (in mm) based on Figure 1

Parameter	Dimension (mm)	Parameter	Dimension
A	150	*N*	15 mm
B	150	*0*	60 mm
C	120	*p*	120°
D	13	*Q*	4 mm
E	90	*R*	8 mm
F	0.9	*s*	4 mm
G	8	*T*	20 mm
H	60	*R1*	0.04
I	60	*R2*	−0.2
J	20	*R3*	0.1
K	15	*R4*	0.05
L	60	*R5*	−0.05
M	25		

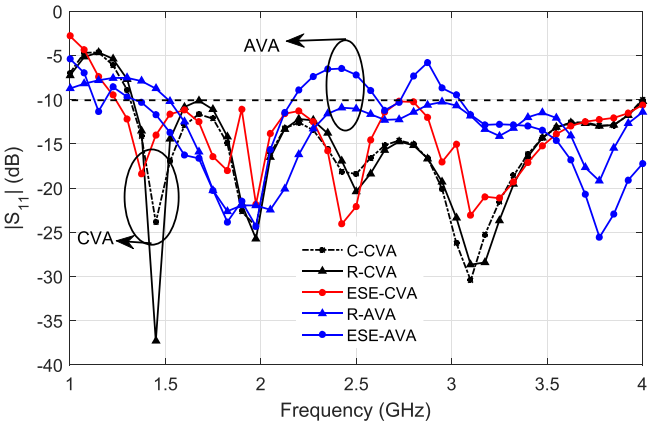

FIGURE 2 Reflection coefficient performance of CVA and AVA. AVA, antipodal Vivaldi antenna; CVA, coplanar Vivaldi antenna [Color figure can be viewed at wileyonlinelibrary.com]

$$C_1 = \frac{y_2 - y_1}{e^{R_n x_2} - e^{R x_1}} \tag{2}$$

$$C_2 = \frac{y_1 e^{R_n x_2} - y_2 e^{R_n x_1}}{e^{R_n x_2} - e^{R_n x_1}} \tag{3}$$

where y is exponential curve and x_1, y_1 (x_2, y_2) are the start (end) points of the tapered slot and C1 and C2 are constant. All the exponential shape for tapered slot and slot edge are determined by setting some opening rate (Rn), as indicated in Table 1.

3 | ANTENNA PERFORMANCE

3.1 | CVA and AVA reflection coefficient and surface current performance

We compare the reflection coefficient performance of the antennas in coplanar (C-CVA, R-CVA, and ESE-CVA) and antipodal (R-AVA and ESE-AVA) configurations, as shown in Figure 2. The first reflection coefficient at −10 dB is obtained from CST simulations for ESE-AVA at 1.14 GHz, ESE-CVA at 1.23 GHz, C-CVA at 1.32 GHz, R-CVA at 1.34 GHz, and R-AVA at 1.51 GHz. From the theory, to get the low end cut off frequency of the Vivaldi element, the element width should be set more than equal to half of the cut off its wavelength.[22] In our design, we just focused on the *L* and *S* band (1-4 GHz) and not optimized below 1.5 GHz. However, if we set the frequency range below 1 GHz, it is possible that some resonance appears. In this simulation, we just presented every 25 data from 1000 data S11 to facilitate the printing of the figure.

CVA and AVA are designed with the same tapered slot value (shown with dash line in the square area in Figure 3) and the same width of transmission line, the ESE AVA antenna provides better performance of reflection coefficient at low end of frequency than the ESE coplanar. But at 3 GHz, Electric field in the tapered slot is stronger in CVA than in AVA, as shown in the comparison between results in Figure 3C,E.

The intensity of electric field at the beginning of tapered slot indicates good resonance at higher frequencies and in the opening mouth of tapered slot indicates good resonance at lower frequencies. Figure 3 shows the surface currents at 3 GHz for all antennas, indicating that, despite the same dimensions, the ESE-CVA has the highest surface current. By exciting the feeding of antenna, it yields electric field and produces higher current distribution. The exponential slot edge traps the propagation of electric field and surface current, leading to an antenna with a higher gain than the one without the exponential slot edge.

However, the intensity of electric field depends on an impedance matching from the feeding to slot line and from the tapered slot to free space. In this paper, we emphasize electric field of antenna only in vertical polarization as shown in Figure 3F. It is shown by vertical E-Field vector plot of C-CVA between two exponential tapered slot. The polarization of Vivaldi antenna depend on its excited feeding and the structure of the Vivaldi patch.

3.2 | CVA and AVA radiation pattern performance

Figure 4 shows the antenna gain at 3 GHz for the coplanar antennas, indicating that ESE-CVA provided the best gain, followed by R-CVA and C-CVA. For antipodal antennas, the ESE-AVA has a larger gain than R-AVA. However, the ESE-AVA has a more asymmetric radiation pattern than the ESE-CVA, as shown in the lower part of Figure 4. Figure 5 shows a comparison of the gain at several frequencies for all antennas, indicating that the best results are obtained with the ESE-CVA. The gains at 3 GHz are 10.74 dB for ESE-CVA, 7.92 dB for R-CVA, 7.90 dB for C-CVA, 7.64 dB for ESE-AVA, and 6.22 dB for R-AVA.

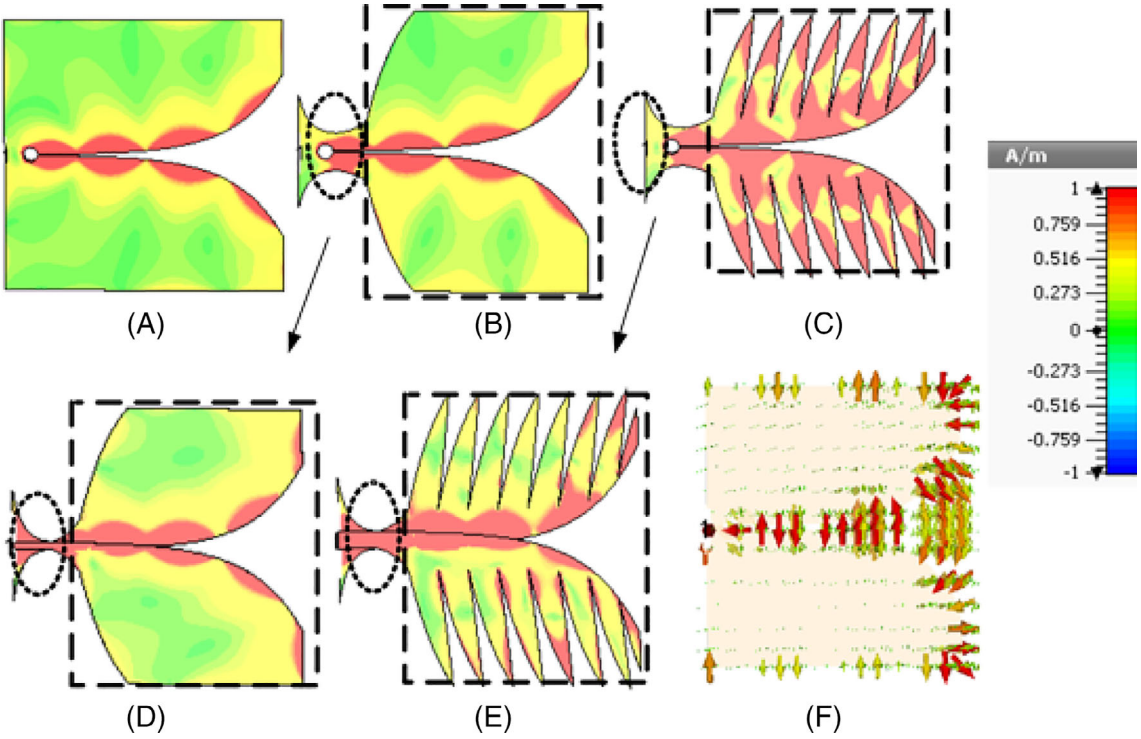

FIGURE 3 Surface current performance for A, C-CVA; B, R-CVA; C, ESE-CVA; D, R-AVA; and E, ESE-AVA; and F, E-Field vector plot of C-CVA. C-CVA, conventional coplanar Vivaldi antenna; ESE-AVA, exponential slot edge antipodal Vivaldi antenna; ESE-CVA, exponential slot edge coplanar Vivaldi antenna; R-AVA, regular antipodal Vivaldi antenna; R-CVA, regular coplanar Vivaldi antenna [Color figure can be viewed at wileyonlinelibrary.com]

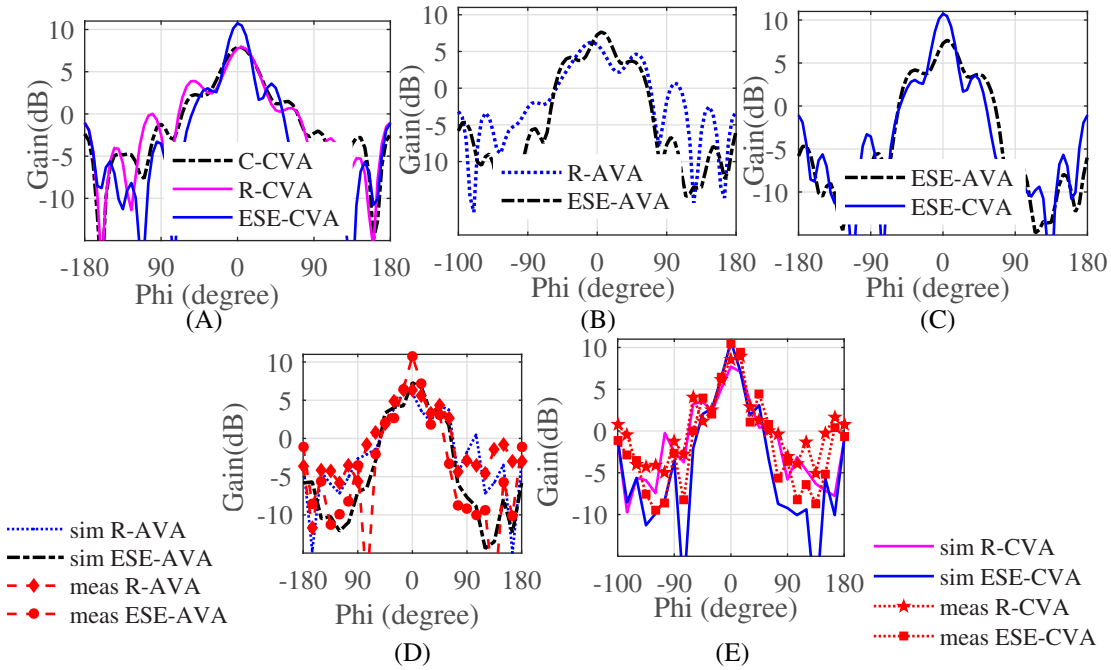

FIGURE 4 Antenna gain at 3 GHz in the E-plane (XY-plane): (A) simulation results of CVA, (B) simulation results of AVA, (C) simulation results of ESE-AVA and ESE-CVA, (D) simulation and measurement results of R-AVA and ESE AVA, and (E) simulation and measurement results of R-CVA and ESE-CVA. ESE-AVA, exponential slot edge antipodal Vivaldi antenna; ESE-CVA, exponential slot edge coplanar Vivaldi antenna; R-AVA, regular antipodal Vivaldi antenna; R-CVA, regular coplanar Vivaldi antenna [Color figure can be viewed at wileyonlinelibrary.com]

Figure 5 shows that Coplanar Vivaldi has lower SLL than AVA. It could be happened because AVA has radiator in the different side of substrate. It interferes the shape of SLL and gain, while coplanar has radiator in the same side of substrate. The CVA has two tapered slots in the same side of the substrate and the feeding of CVA is located on the

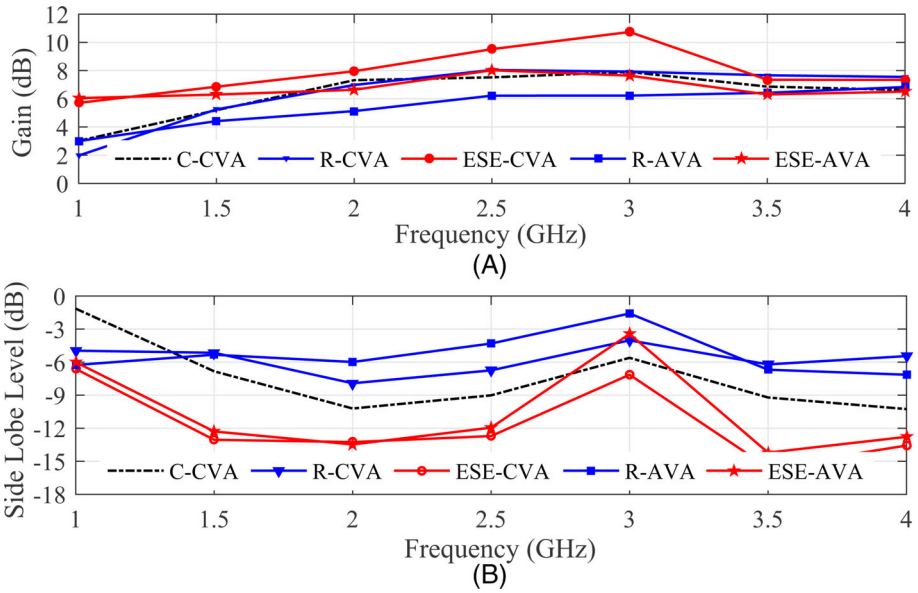

FIGURE 5 A, Gain and B, SLL performance of the antennas [Color figure can be viewed at wileyonlinelibrary.com]

reverse side of substrate. If the feeding has matching impedance with the slot line, it yields resonance between two tapered slots. In CVA, electric field propagates between two tapered slots in the same side of substrate. CVA can be designed with specific feeding shape and it influences the CVA bandwidth. ESE-CVA also has high gain because the electric field is strengthened by the exponential slot edge. In AVA, current from feeding propagates directly from the transmission line in the straight line to the tapered slot, which is located on the opposite side of substrate. In this case, we compare all Vivaldi antennas with the same width of transmission line, and the CVA provides better performance than AVA.

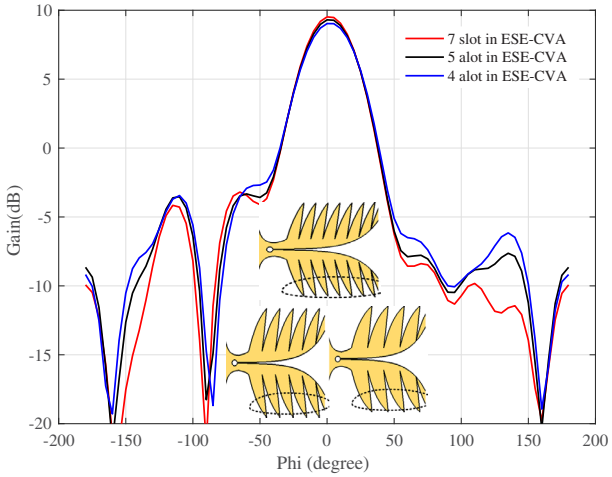

FIGURE 6 Radiation pattern ESE-CVA with varying the number of slot at 2.5 GHz. ESE-CVA, exponential slot edge coplanar Vivaldi antenna [Color figure can be viewed at wileyonlinelibrary.com]

4 | ESE-CVA: OPTIMIZATION AND MEASUREMENT RESULTS

4.1 | ESE-CVA radiation pattern

ESE-CVA provides the best performance in radiation pattern and bandwidth, as discussed in the previous section. However, there are several parameters to design the slot edge that affect radiation pattern performance. The radiation pattern of the ESE-CVA could be optimized by varying some parameters of the exponential slot edge. The number of exponential slot edges interferes on gain, side lobe level, back lobe, and beam width. From simulation results at 2.5 GHz as the center frequency, as shown in Figure 6, the ESE-CVA with seven slots has the main lobe of 9.5 dB, SLL of −12.7 dB, and beam width of 39.8°. On the other hand, the antenna with five slots has the main lobe of 9.3 dB, SLL of −12.6 dB, and beam width of 40.7°, whereas for four slots has the main lobe of 9 dB, SLL of −12.5 dB, and beam width of 42.2°. Therefore, more slots can increase the main lobe and reduce SLL, but provide a larger beam width. This occurred because the electric field resonates between slot edges, improving the radiation pattern.

The height of ESE from the center of tapered slot, shown in Figure 7A, and represents the slope of exponential slot edge, shown in Figure 7B, interfere with the radiation pattern performance. When the height of ESE (h_A) is 15 mm, the antenna gain is 10.7 dB and SLL −7.1 dB. On the other hand, when h_B is 50 mm, the antenna gain is 8.1 dB and SLL −5.4 dB. The shorter the height of slot edge to the center of the opening tapered slot, as shown in Figure 7A, the more electric field induces the slot edge and enhances the gain. For the antenna with $R = 0.04$, the main lobe is 10.7 dB, SLL is −7.1 dB, and squint is 0°, while for $R = 0.001$, the main lobe is 8.8 dB, SLL is −5.6 dB, and the

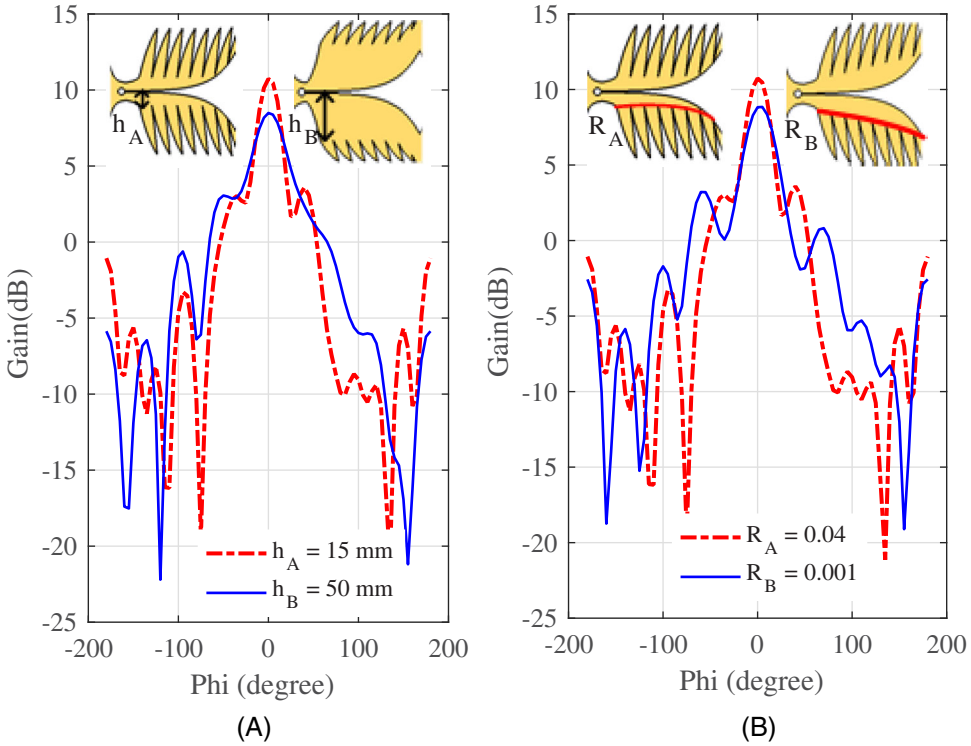

FIGURE 7 Gain of ESE-CVA by varying depth of slot and slope of ESE at 2.5 GHz. ESE-CVA, exponential slot edge coplanar Vivaldi antenna [Color figure can be viewed at wileyonlinelibrary.com]

squint is 5°. This indicates that the slope of ESE could control radiation pattern performance. It shows that the shorter height (*h*) of slot edge from center of tapered slot and higher opening rate (R) of slot edge improve the gain, SLL performance, and the squint performance of the main lobe.

4.2 | Surface current of ESE-CVA

The surface current performance for ESE-CVA with different heights of slot edge from the center of the element, different number of slot edge, and different slope of slot edge is shown in Figure 8. Higher intensity of electric current, represented by surface current distribution, is reached for shorter height (hA) of slot edge, as shown in Figure 8A, while higher height (hB) of slot edge yields less surface current distribution, as shown in Figure 8B. Higher densities of surface current, which resulted from electric field in the mouth opening of the tapered slot, appears in the slot edge of CVA that has higher depth of slot edge. Higher depth in the slot edges means shorter height (hA) of slot edge to the center of tapered slot. However, for short depth of slot edge only shows a small surface current at the corner of the slot edge, represented in red color in Figure 8B.

Figure 8A,C show a comparison on the surface current for the element with different number of slot edges. CVAs in Figure 8A,C are designed with the height of slot edge $h_A = 15$ mm and slope of slot edge $R_A = 0.04$. Those CVA have the same height of slot edge to the center of tapered slot, but they have different number of slot edge.

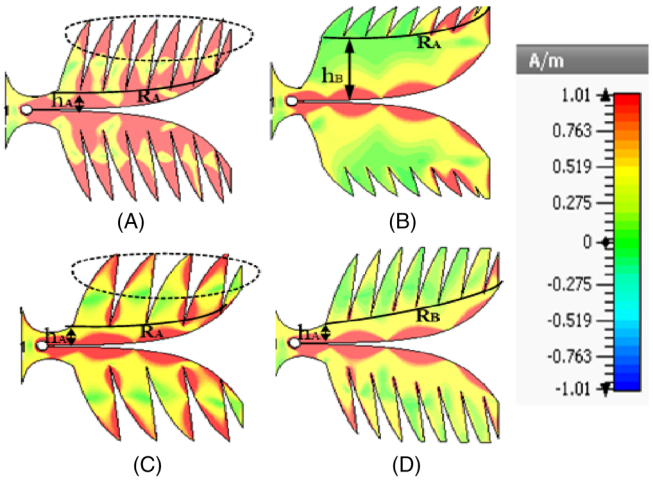

FIGURE 8 Surface current of CVA at 3 GHz with; A, number of slot = 7, depth of slot = 15 mm $R = 0.04$; B, number of slot = 7,depth of slot = 50 mm $R = 0.04$; C, number of slot = 4, depth of slot 15 mm $R = 0.04$; and D, number of slot = 7, depth of slot 15 mm $R = 0.01$. CVA, coplanar Vivaldi antenna [Color figure can be viewed at wileyonlinelibrary.com]

At 3 GHz, the CVA with seven slot edges presents the maximum surface current in the most part of all sections, as shown in Figure 8A, while the CVA with smaller number of slot edges presents less portion of surface current, as shown in Figure 8C. Therefore, more slot edges lead to more electric field induced in the slot gap and it also yield surface currents trapped in the slot edge. An increase in the number of exponential slots increases surface current in CVA.

Surface current performance for CVA with different slope is shown in Figure 8A,D, designed with $R_A = 0.04$ and $R_B = 0.01$, respectively. A higher slope of tapered slot edge to the center of the antenna increases performance of surface current. In the middle and towards the end of mouth opening of tapered slot, higher slope (R_A) has smaller distance of slot edge from opening tapered slot. It conversely for smaller slope (R_B) that has longer distance of slot edge from opening of tapered slot. The slope of slot edge influences the spacing of slot edge to the mouth opening of tapered slot in the middle and in the end of tapered slot and it causes the flowing of surface current to the slot edge.

4.3 | Measurement results of CVA and AVA

Figure 9 shows a comparison of simulations and measurements of the reflection coefficient (S11) for regular (R) and exponential slot edge (ESE) of CVA, whereas Figure 10 clarifies simulations and measurements of R-AVA and ESE-AVA. CVA provides better performance in bandwidth than AVA, especially at low end of the frequency band. Table 2 shows the values of gain, SLL, squint, and the lowest frequency that occupies reflection coefficient performance below −10 dB, between simulations and measurements.

Table 2 presents about the comparison of R-AVA, ESE-AVA, C-CVA, R-CVA and ESE-CVA gain, SLL, squint and the lowest frequency at 2.5 and 3 GHz. It indicates that ESE-CVA gets the best performance of gain, SLL, and squint at 2.5 and 3 GHz, even though the lowest of frequency band is reached for ESE-AVA. High SLL will decrease the antenna gain and it can influence the signal reception quality because it increase interferences of reception. It results false target detection. By modifying the

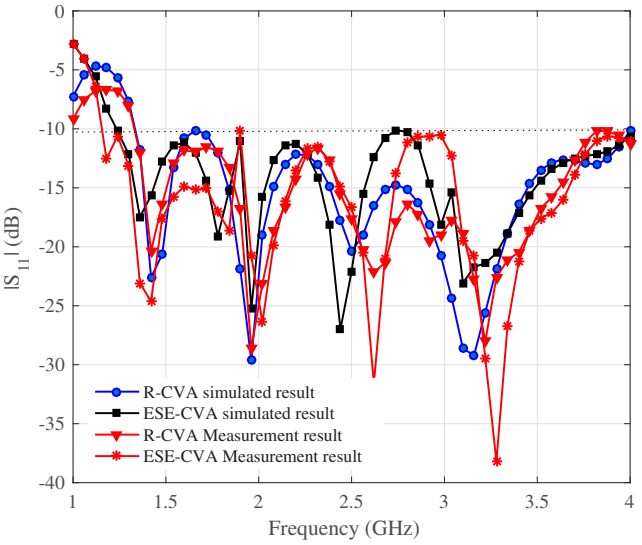

FIGURE 9 Simulation and measurement results of R-CVA and ESE-CVA on S_{11} as a function of frequency. ESE-CVA, exponential slot edge coplanar Vivaldi antenna; R-CVA, regular coplanar Vivaldi antenna [Color figure can be viewed at wileyonlinelibrary.com]

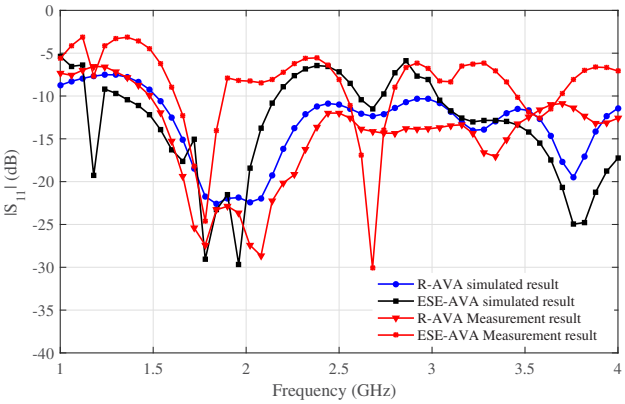

FIGURE 10 Simulation and measurement results of R-AVA and ESE-AVA on S_{11} as a function of frequency. ESE-AVA, exponential slot edge antipodal Vivaldi antenna; R-AVA, regular antipodal Vivaldi antenna [Color figure can be viewed at wileyonlinelibrary.com]

corrugated slot, the radiator, feeding shape or adding some structure in opening mouth of antenna element, it will allow lowering the SLL Table 2 shows that CVA has lower SLL than AVA and by adding exponential corrugated slot it can reduce the SLL, at 2.5 GHz as center frequency, antenna element has the lowest SLL as −12.71 than at 3 GHz.

Table 3 shows the comparison of our proposed configuration and those from the literature. It shown that mostly researched only discussed for one type of vivaldi element that is Antipodal Vivaldi Antenna (AVA). Here, we show clearly that the Coplanar configuration presents a major improvement on the results, as compare to the Antipodal configuration with the same substrate dimensions and similar shape of the exponential edge and tapered slot. In specific dimension and frequency,[22] shown in the last row of Table 3, our proposed structure provided a wider bandwidth and higher gain than those in the literature.

Figure 11 shows the AVA and CVA fabricated antennas with regular and exponential slot edges. Figure 11A-C shows the front view of R-AVA, R-CVA and ESE-CVA, respectively, while Figure 11D-F shows its respective feeding in back views.

4.4 | Near Field Measurement Application

Figure 12 displays near field measurement of CVA with four different treatment that is, (a) CVA with thin board, (b) CVA with head phantom made from styrofoam, (c) CVA with thick wood, (d) CVA with thin Styrofoam, and (e) AVA with head phantom. In Figure 12, the styrofoam has epsilon er = 1,1, however the wood has er = 2.4. The environment object of measurement can be shown in Figure 12A-E with the target in Figure 12F,H. The measured S-parameter used Copper Mountain Cobalt series c1220 Vector Network Analyzer which is connected to the CVA antenna in Figure 12A-D,G whereas in Figure 12E connected to AVA antenna. In the first row of Figure 13 shows

TABLE 2 Comparison between antennas: gain, SLL, squint from simulations, and measurements

	Gain (dB)		SLL (dB)		Lowest frequency		
Fre (GHz)	**2.5**	**3**	**2.5**	**3**	**Sim. result**	**Meas. result**	**Squint**
R-AVA	6.2	6.2	−4.31	−1.58	1.52	1.48	−5
ESE-AVA	8.02	7.64	−11.94	−3.44	1.14	1.62	−5
C-CVA	7.51	7.9	−9.02	−5.61	1.32	1.2	0
R-CVA	8.04	7.93	−6.74	−4.02	1.34	1.34	5
ESE-CVA (proposed antenna)	9.52	10.74	−12.71	−7.14	1.23	1.16	0

Abbreviations: C-CVA, conventional coplanar Vivaldi antenna; ESE-AVA, exponential slot edge antipodal Vivaldi antenna; ESE-CVA, exponential slot edge coplanar Vivaldi antenna; R-AVA, regular antipodal Vivaldi antenna; R-CVA, regular coplanar Vivaldi antenna.

TABLE 3 Comparison the proposed and literature studied

Reference, type, technic	Size ($W \times L \times h$)	Subs. permittivity	Bandwidth (GHz)	Gain
2, CVA, –	260 × 254	duroid 5880 er = 2.2	0.7-2.7	7.4 dBi
8, AVA, slit edge and trapezoid lens	40 × 90 × 0.508	Roger RO4003C er = 3.38	3.4-40	14.6 dB (40GHz)
9, DAVA, edge slit	70 × 166 × 0.762	RO4350 er = 3.48	4.7-20	15 dB(16 GHz)
11, AVA,taper slot edge	48 × 60	FR4, er = 4.6	2.5-15	10 dB (7.5 GHz)
12, AVA, comb slit edge	120 × 202 × 0.508 mm^2	R04003C er = 3.38	1.65-18	10.3 (3 GHz)
14, AVA	80 × 60 × 1.6	FR4 er = 4.3	3.1-10.6	copol/xpol20 dB
16, CVA, side slot	88 × 751.57 mm	Duroid 5870	1.54-7	9.8 dBi (6 GHz)
17, AVA, exponential slot edge	36.3 × 59.8 × 0.64	RO3206 er = 6.15	5.6-11	8.3 dB (6 GHz)
18, AVA	40 × 90 × 0.508	RO4003C er = 3.38	3.4-40	14.3 (40 GHz)
19, AVA, fren leaf	50.8 × 62	FR4,er = 4.4	1.3-20	10 dBi
22, AVA	150 × 150	FR4 ER = 4.3	1.5-3.5	7.9 dB
Our purpose, CVA	150 × 150	FR4 ER = 4.6	1.23-4	10.7 dB or 11.9 dBi (3 GHz)

Abbreviations: AVA, antipodal Vivaldi antenna; CVA, coplanar Vivaldi antenna.

different characteristic of S11 with target behind of the object as observed in Figure 12A,D and target inside of the object in Figure 12B,C,E,G. Thin board has thickness 8 mm as shown in Figure 12A and thin styrofoam has thickness 29 mm as displayed in Figure 12D. In the first row of Figure 13, the thin board and thin Styrofoam has worse S parameter than head phantom and thick wood for CVA, but the worst S11 is shown for AVA antenna as shown in the first row of Figure 13E. Object with thin thickness will have smaller distance between target and the antenna, furthermore it influences S parameter measurement performance.

The S11 data from VNA have been imported from touchstone block CST Design Studio, and converted to time domain reflectometry (TDR). TDR signal from post processing in CST related to Inverse Fourier Transform and shown in the second row of Figure 13. The time sampling is set as 30 ns for all the TDR signal. The target in Figure 12E is placed in the object of Figure 12A,B,E, while the target in Figure 12H is placed in the object in Figure 12C,D. It shows different characteristic of signal from object with target in the second row of Figure 13 and object without target as shown in the third row of Figure 13. The subtraction signal in the second and third row resulted the signal in the fourth row in Figure 13.

However the absolute of the subtraction signal yields output in the fifth row of Figure 13. It shows that thin board have higher amplitude of target signal than in thin Styrofoam. It also shows that the head phantom can detect target with higher signal than in the thick wood. With the same size of antenna, CVA with head phantom has higher detection of target signal than AVA with head phantom as shown in the last signal in Figure 13B,E. It happened because CVA has better performance of S11 than AVA as shown in the first row Figure 13B,E. It is also observed that object with board or wood has deployment of signal than object with Styrofoam. Thick wood as shown in Figure 12G has more solid of particle than others. Object with higher dense of particle and further distance of target will have smaller amplitude of signal and higher deployment of target signal.

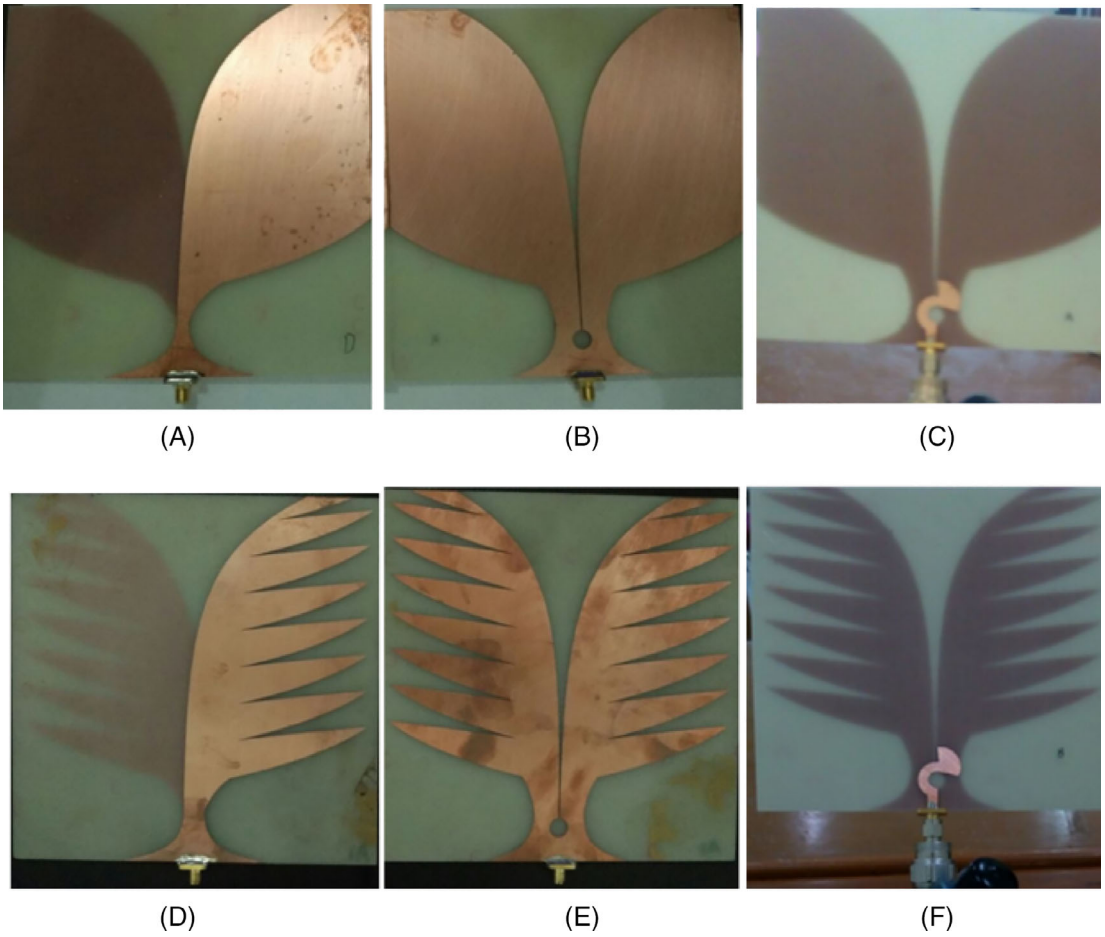

FIGURE 11 Fabricated antennas: A, R-AVA front view; B, R-CVA front view; C, R-CVA back view; D, ESE-AVA front view; E, ESE-CVA front view; and F, ESE-CVA back view. ESE-AVA, exponential slot edge antipodal Vivaldi antenna; ESE-CVA, exponential slot edge coplanar Vivaldi antenna; R-AVA, regular antipodal Vivaldi antenna; R-CVA, regular coplanar Vivaldi antenna [Color figure can be viewed at wileyonlinelibrary.com]

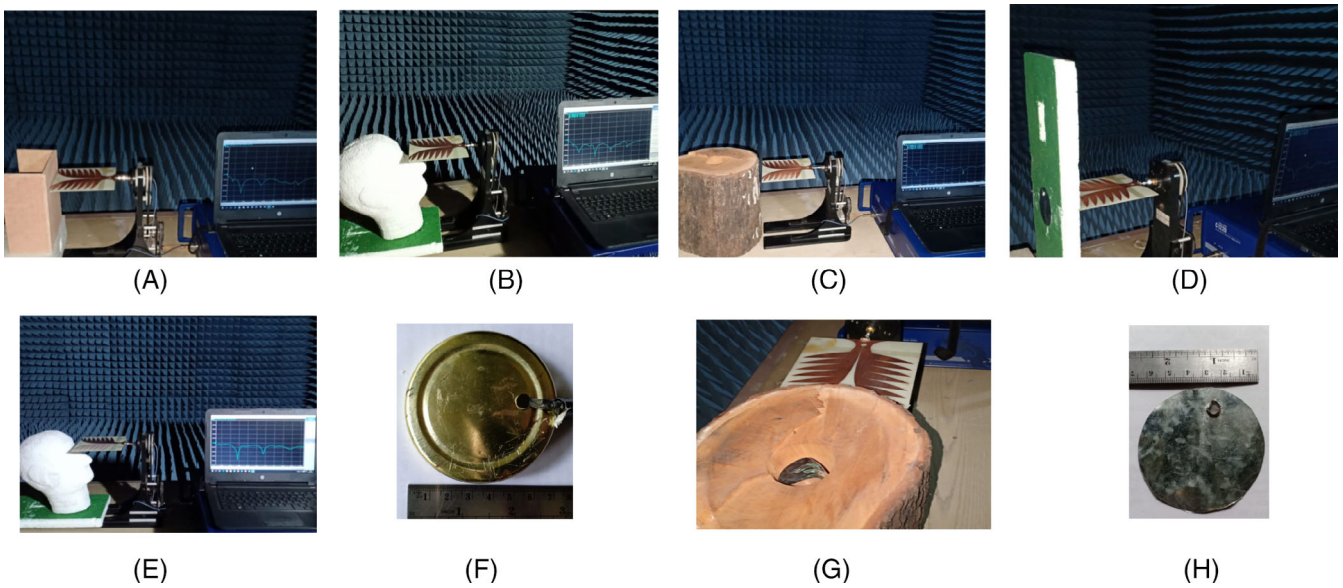

FIGURE 12 Fabricated antennas: A, R-AVA front view; B, R-CVA front view; C, R-CVA back view; D, ESE-AVA front view; E, ESE-CVA front view; and F, ESE-CVA back view. ESE-AVA, exponential slot edge antipodal Vivaldi antenna; ESE-CVA, exponential slot edge coplanar Vivaldi antenna; R-AVA, regular antipodal Vivaldi antenna; R-CVA, regular coplanar Vivaldi antenna [Color figure can be viewed at wileyonlinelibrary.com]

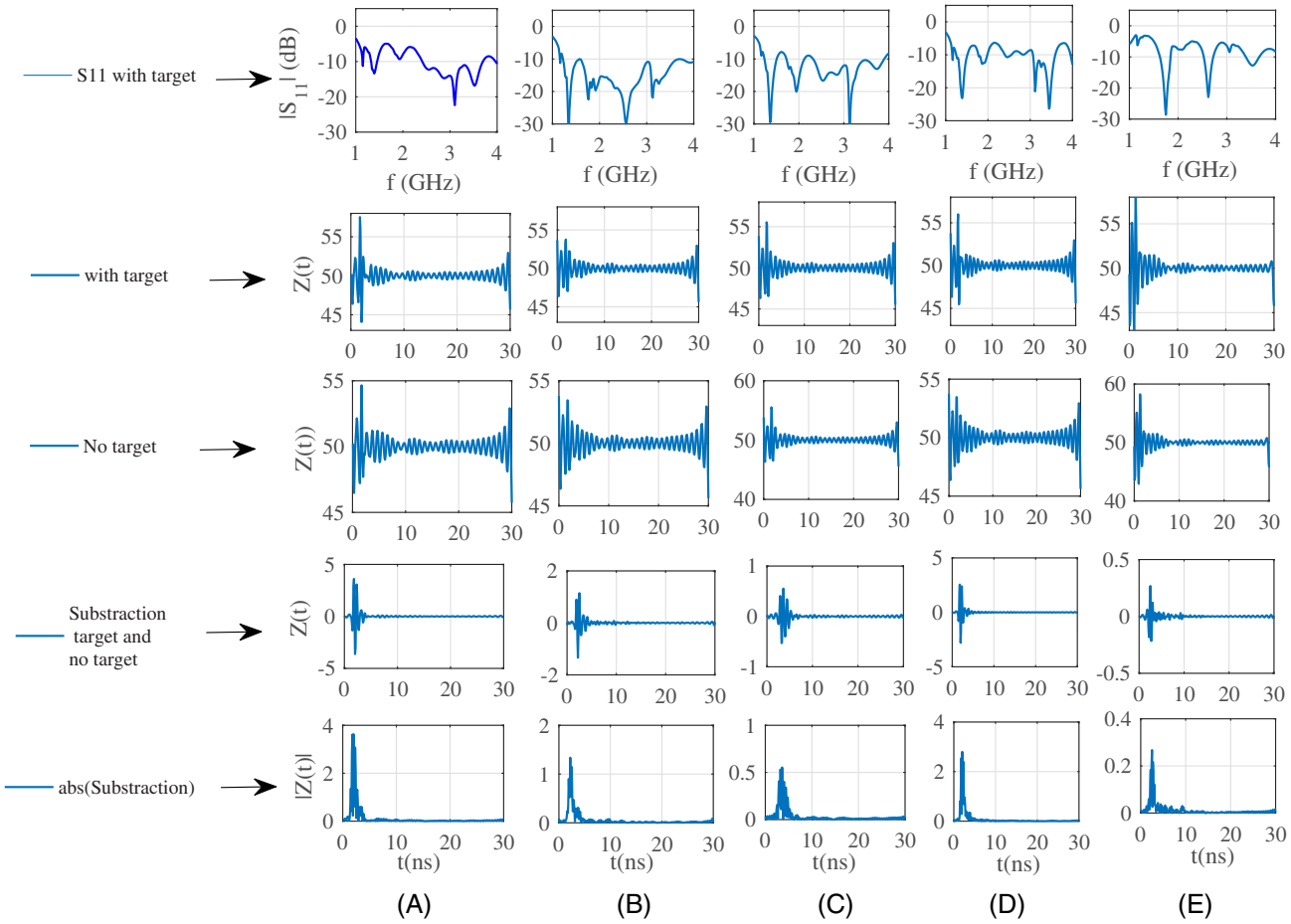

FIGURE 13 Measurement result of S11 with target in the first row, TDR signal for object with target in the second row, TDR signal for object without target in the third row, Substraction object with target and without target in fourth row and the magnitude of the substraction in the fifth row for object:: (A) CVA with thin board, (B) CVA with head phantom from styrofoam, (C) CVA with thick wood, (D) CVA with thin styrofoam, and (E). AVA with head phantom from styrofoam. AVA, antipodal Vivaldi antenna; CVA, coplanar Vivaldi antenna; TDR, time domain reflectometry [Color figure can be viewed at wileyonlinelibrary.com]

5 | CONCLUSION

We compared the properties of Vivaldi antennas consisting of R-AVA, ESE-AVA, C-CVA, R-CVA, and ESE-CVA with the same dimensions of substrate and similar shape of exponential edge and tapered slot. The results indicate that ESE-CVA provides the best performance of gain and side lobe level. Although the feeding and substrate is designed with the same width, AVA and CVA have different performance. The corrugated slot, radiator and the feeding shape influences the performance of return loss and radiation pattern. The number of exponential slot edges, the distance of exponential slot edge to the center of the antenna and the slope of exponential slot edge can control radiation pattern performance. ESE-CVA has better performance of radiation pattern compared to others. Gain improvement is obtained for ESE-CVA of 3.02 dB and SLL of −2.53 dB at 3 GHz when compared to ESE-AVA. Object with higher solid particle and wider distance from the antenna yield worse detection of target signal from near field experimental measurement. With the same size of antenna element and the same object and target, CVA has better performance than AVA.

ORCID

N. Nurhayati https://orcid.org/0000-0002-3428-8570
Alexandre M. De Oliveira https://orcid.org/0000-0002-7493-7117

REFERENCES

[1] Z. N. Chen, M. J. Ammann, and X. Qing, "Planar Antennas," *IEEE Microw Mag*, no December, pp. 63–73, 2006, 7.

[2] Cellular G, Applications B, Dong Y. Vivaldi antenna with pattern diversity for 0.7 to 2.7 GHz Cellular band Applications. *IEEE Antennas Wirel Propag Lett*. 2018;17(2):247-250.

[3] X. Liu, M. Serhir, A. Kameni, M. Lambert, and L. Pichon, "Buried targets detection from synthetic anc measured B-scan ground penetrating radar data," *11th Eur. Conf. Antennas Propagation, EUCAP* 2017, pp. 1726–1730, 2017.

[4] Hall BPS, Ieee F, Gardner P, Ieee SM, Faraone A, Ieee SM. Antenna requirements for software defined and cognitive radios. *Proc IEEE*. 2012;100(7):2262-2270.

[5] Chandra R, Zhou H, Balasingham I, Narayanan RM. On the opportunities and challenges in microwave medical sensing and imaging. *IEEE Trans Biomed Eng*. 2015;62(7):1667-1682.

[6] Gaetano D, McEvoy P, Ammann MJ, Browne JE, Keating L, Horgan F. Footwear antennas for body area telemetry. *IEEE Trans Antennas Propag*. 2013;61(10):4908-4916.

[7] Reid EW, Ortiz-Balbuena L, Ghadiri A, Moez K. A 324-element vivaldi antenna array for radio astronomy instrumentation. *IEEE Trans Instrum Meas*. 2012;61(1):241-250.

[8] Moosazadeh M, Kharkovsky S, Case JT. Microwave and millimetre wave antipodal Vivaldi antenna with trapezoid-shaped dielectric lens for imaging of construction materials. *IET Microw Antennas Propag*. 2016;10:301-309.

[9] Zhang Y, Member S, Li E, Wang C, Guo G. Radiation enhanced Vivaldi antenna with double-antipodal structure. *IEEE Antennas Propag Lett*. 2017;16:561-564.

[10] Sun M, Chen ZN, Qing X. Gain enhancement of 60-GHz antipodal tapered slot antenna using zero-index metamaterial. *IEEE Trans Antennas Propag*. 2013;61(4):1741-1746.

[11] Fei P, Jiao YC, Hu W, Zhang FS. A miniaturized antipodal vivaldi antenna with improved radiation characteristics. *IEEE Antennas Wirel Propag Lett*. 2011;10:127-130.

[12] Moosazadeh M, Kharkovsky S, Case JT, Samali B. Antipodal Vivaldi antenna with improved radiation characteristics for civil engineering applications. *IET Microw Antennas Propag*. 2017;11:796-803.

[13] Ludlow P, Fusco VF. Antipodal Vivaldi antenna with tuneable band rejection capability. *IET Microw Antennas Propag*. 2011;5(3):372.

[14] Natarajan R, Kanagasabai M, Gulam Nabi Alsath M. Dual mode antipodal Vivaldi antenna. *IET Microw Antennas Propag*. 2016; 10(15):1643-1647.

[15] N. T. Nguyen et al., "Wideband Vivaldi antenna array with mechanical support and protection radome for land-mine detection radar," *45th Eur. Microw. Conf. Proceedings, EuMC*, pp. 1559–1562, 2015.

[16] Çayören M, Abbak M, Akduman İ. Microwave breast phantom measurements with a cavity-backed Vivaldi antenna. *IET Microw Antennas Propag*. 2014;8(13):1127-1133.

[17] De Oliveira AM, Perotoni MB, Kofuji ST, Justo JF. A palm tree antipodal Vivaldi antenna with exponential slot edge for improved radiation pattern. *IEEE Antennas Wirel Propag Lett*. 2015;14: 1334-1337.

[18] Moosazadeh M, Kharkovsky S. A compact high-gain and front-to-Back ratio elliptically tapered antipodal Vivaldi antenna with trapezoid-shaped dielectric lens. *IEEE Antennas Wirel Propag Lett*. 2016;15:552-555.

[19] Biswas B, Ghatak R, Poddar DR. A Fern fractal leaf inspired wideband antipodal Vivaldi antenna for microwave imaging system. *IEEE Trans Antennas Propag*. 2017;65(11):6126-6129.

[20] Nurhayati, G. Hendrantoro, and E. Setijadi, "Comparison Study of S-Band Vivaldi-Based Antennas," in 2016 IEEE Region 10 Symposium (TENSYMP), 2016, pp. 188–193.

[21] Nurhayati N, Hendrantoro G, Fukusako T, Setijadi E. Mutual coupling reduction for UWB coplanar Vivaldi array by truncated and corrugated slot. *IEEE Antennas Wirel Propag Lett*. 2018;17(12): 2284-2288.

[22] De Oliveira AM, Justo JF, Serres AJR, et al. Ultra-directive palm tree Vivaldi antenna with 3D substrate lens for -biological near-field microwave reductions. *Microwave Opt Technol Lett*. 2018; 61:713-719. https://doi.org/10.1002/mop.31618.

How to cite this article: Nurhayati N, De Oliveira AM, Justo JF, Setijadi E, Sukoco BE, Endryansyah E. Palm tree coplanar Vivaldi antenna for near field radar application. *Microw Opt Technol Lett*. 2019;1–11. https://doi.org/10.1002/mop.32127

Microwave and Optical Technology Letters

Country	United States - SIR Ranking of United States
Subject Area and Category	Engineering Electrical and Electronic Engineering Materials Science Electronic, Optical and Magnetic Materials Physics and Astronomy Atomic and Molecular Physics, and Optics Condensed Matter Physics
Publisher	John Wiley & Sons Inc.
Publication type	Journals
ISSN	10982760, 08952477
Coverage	1988-ongoing
Scope	Microwave and Optical Technology Letters provides quick publication (3 to 6 month turnaround) of the most recent findings and achievements in high frequency technology, from RF to optical spectrum. The journal publishes original short papers and letters on theoretical, applied, and system results in the following areas. - RF, Microwave, and Millimeter Waves - Antennas and Propagation - Submillimeter-Wave and Infrared Technology - Optical Engineering All papers are subject to peer review before publication
	Homepage
	Join the conversation about this journal

68

H Index

Quartiles

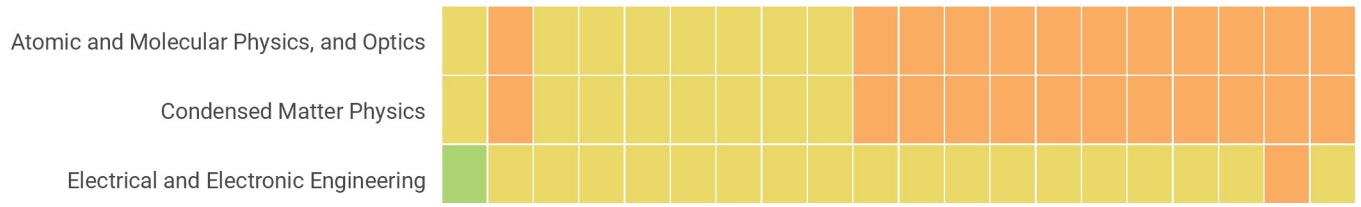

H

SJR

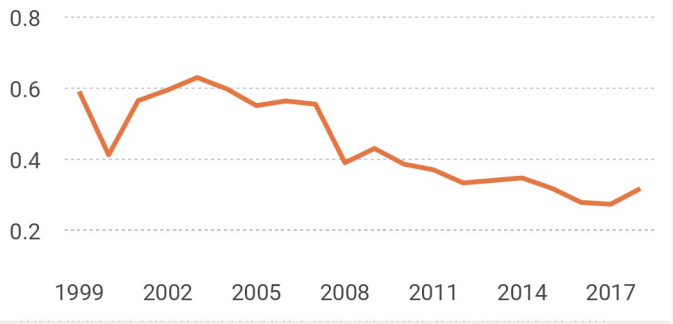

Citations per document

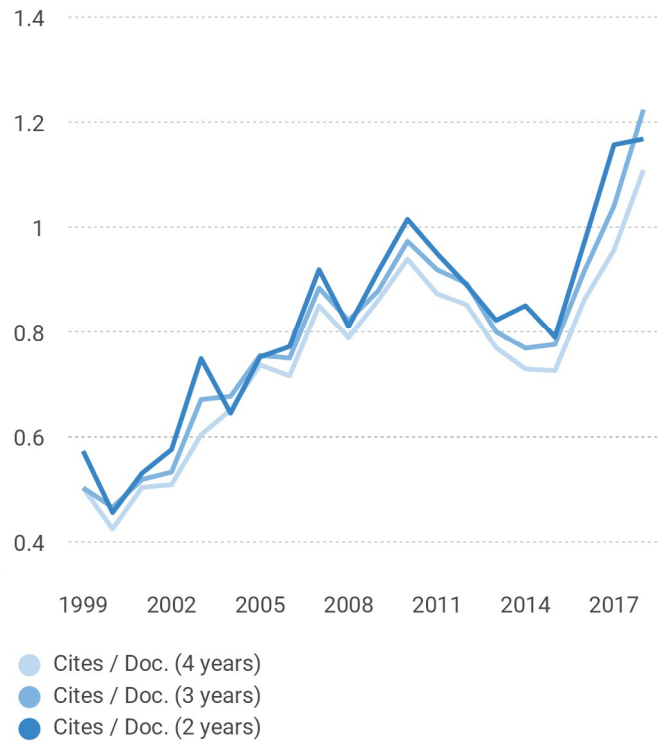

Total Cites Self-Cites

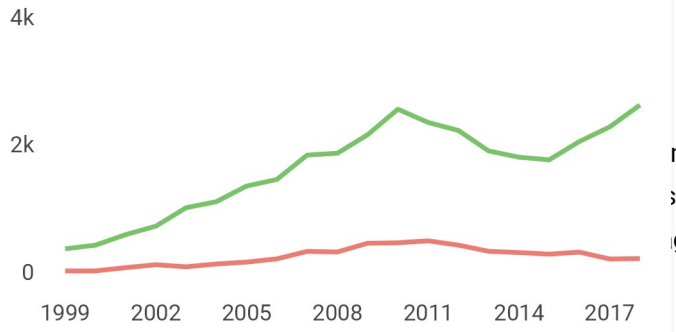

External Cites per Doc Cites per Doc

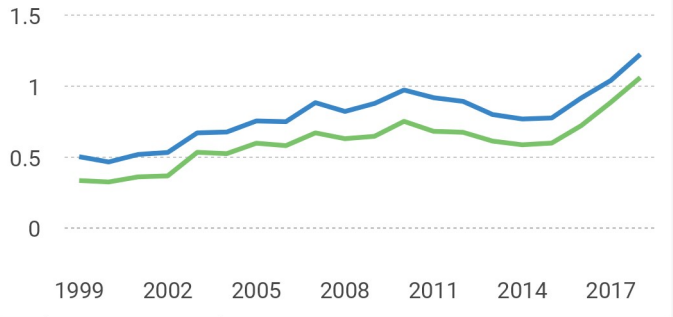

% International Collaboration

(will not be published)

Citable documents Non-citable documents

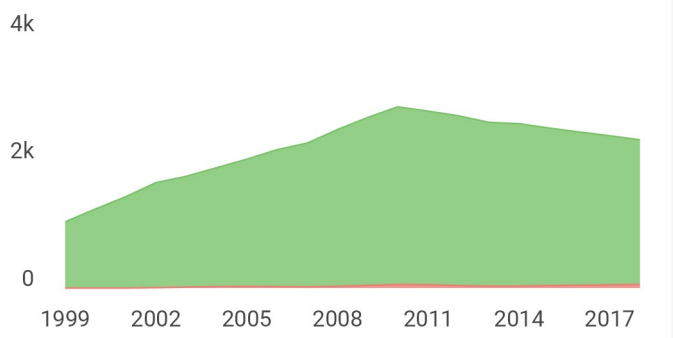

Cited documents Uncited documents

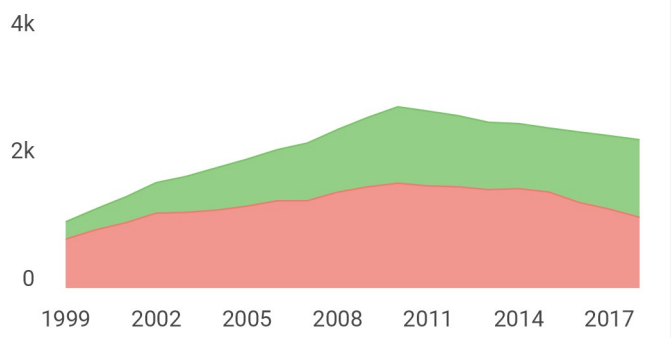

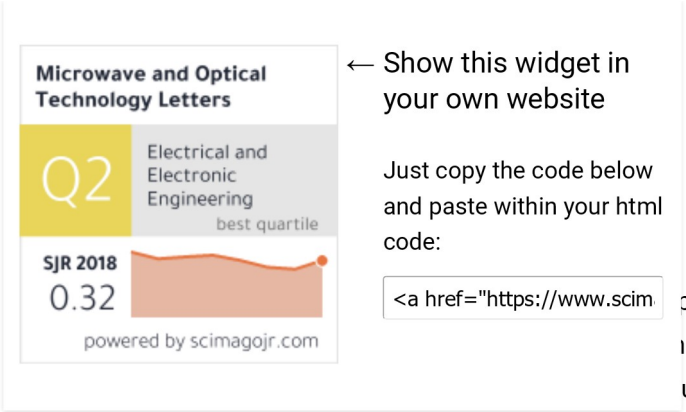

possibility to dialogue through comments linked to a general doubts about the processes of publication in the ublication of papers are resolved. For topics on particular articles, maintain the dialogue through the usual channels with your editor.

Developed by: Powered by:

Follow us on @ScimagoJR

EST MODUS IN REBUS
Horatio (Satire 1,1,106)